DE GRUYTER OPEN

Int. J. of Applied Mechanics and Engineering, 2015, vol.20, No.2, pp.345-372
DOI: 10.1515/ijame-2015-0023

THE FUNDAMENTAL SOLUTIONS FOR THE STRESS INTENSITY FACTORS OF MODES I, II AND III. THE AXIALLY SYMMETRIC PROBLEM

B. ROGOWSKI
Department of Mechanics of Materials
Lodz University of Technology
Al. Politechniki 6, 90 – 924 Lodz, POLAND
E-mail: bogdan.rogowski@p.lodz.pl

The subject of the paper are Green's functions for the stress intensity factors of modes I, II and III. Green's functions are defined as a solution to the problem of an elastic, transversely isotropic solid with a penny-shaped or an external crack under general axisymmetric loadings acting along a circumference on the plane parallel to the crack plane. Exact solutions are presented in a closed form for the stress intensity factors under each type of axisymmetric ring forces as fundamental solutions. Numerical examples are employed and conclusions which can be utilized in engineering practice are formulated.

Key words: cracks, Green's functions, stress intensity factors, analytical solution, mode I, II and III loading conditions, transversely isotropic.

1. Introduction

The basic solutions, related among other to multifield materials, are Green's functions, which were proposed by George Green first in 1828. There are two different analysis processes for the solutions in the science literature. One has focused on displacement, electric potential and magnetic potential, constructing the equilibrium equations. The second has emphasized on equilibrium equations of stresses, electric displacements and magnetic inductions and compatibility equations for strains. There are Stroh's formalism (1958) and Lekhnitskii's approach (1963), for example. On the other hand, there are three commonly used methods in analyzing boundary effects the theoretical solution, the numerical solution and the experiment. But, appropriate Green's functions for the stress intensity factors, not appear up till now since this problem is a specific task.

It is easily understood that the point force continuously distributed in radial (Fig.2) and axial (Fig.4) direction along a ring around the axis of symmetry gives the fundamental solutions for tension problems and those distributed in circumferential direction (Fig.3) give the fundamental solutions for torsion problems. The problems of the cracks treated in the present study are solved by using three types of axisymmetric ring forces as fundamental solutions. Modes I, II and III stress intensity factors derived in this paper are in terms of elementary functions and need no further elaboration. The results presented for general cases are new, some of those relating to special cases of isotropic or transversely isotropic solids with crack surface tractions are known (see Murakami (1987), Rogowski (1986), for example). Livieri nad Segala (2014) obtained in analytical form the stress intensity factor of mode I using of the Oore – Burns weight function (1980). Recently, Green's function for an uncracked piezoelectric medium was presented by Chung (2014).

Nowacki *et al*. (2001; 2002) obtained exact solutions for a piezoelectric layer – substrate structure in the form of Fourier integrals with detailed discussions on the convergence. Ting (2007; 2008) constructed Green's function for an anisotropic piezoelectric half – space bonded to a thin piezoelectric layer subjected to a generalized line force and a generalized line dislocation. The Stroh formalism is adapted and the solutions are explicitly given in elaborations by Chung and Nowacki *et al.*

This article presents in a closed form new influence functions of a unit ring loadings on the displacements and stresses for internal and external cracks and three boundary value problems of fracture mechanics for a transversely isotropic medium. All these results are presented in terms of elementary functions. It is well known that Green's functions play a major role in solving boundary value problems in integrals of different areas of mathematical physics, including fracture mechanics (see monographs by Rogowski 2014a; 2014b).

2. Basic equations

In this study we use cylindrical coordinates and denote them by (r,θ,z) or (x_i, $i=1$, 2, 3). Let a penny-shaped crack or an external crack be located in the plane $z = 0$ of a homogeneous and transversely isotropic elastic solid.

The penny-shaped crack occupies the region $0 \le r \le a$ ($z = 0$) and the external crack occupies the region $r \ge a$ ($z = 0$). Both sides of the cracks are stress free. The half- space $z \ge 0$ is subjected to axisymmetric body forces

$$F_i = \frac{l_i}{2\pi r}\delta(r-b)\delta(z-h) \qquad (i=1,3),$$
$$F_2 = \frac{l_2}{2\pi r^2}\delta(r-b)\delta(z-h) \qquad (i=2), \tag{2.1}$$

distributed along the circumference of a circle ($r = b$, $z = h$) in the interior of the solid, where $\delta(\ )$ is a Dirac delta function and F_1, F_2, F_3 are a radial force, a torsional force and an axial force, respectively, as shown in Figs 2, 3 and 4.

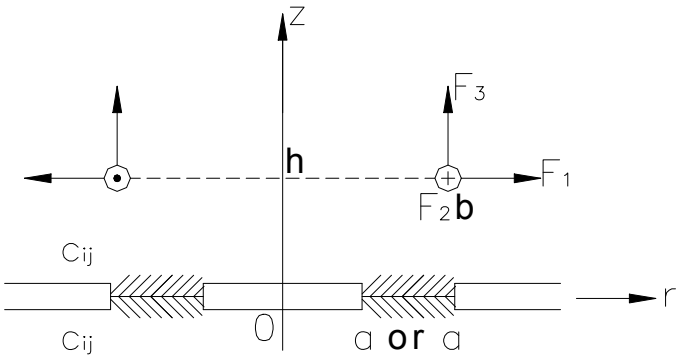

Fig.1. A transversely isotropic elastic solid with a penny-shaped or external crack.

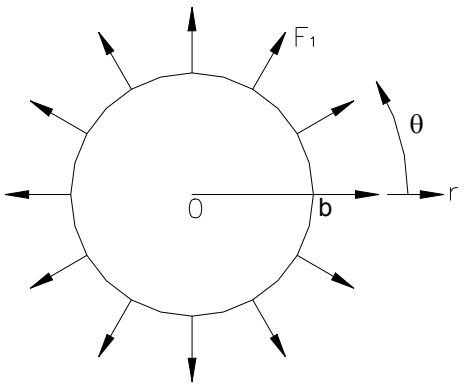

Fig.2. A radial force acting along a circle.

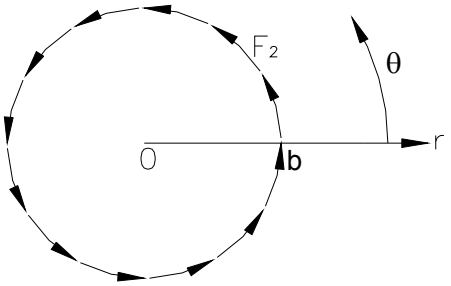

Fig.3. A torsional force acting along a circle.

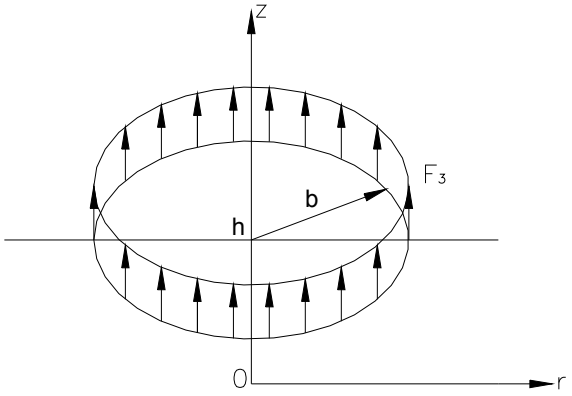

Fig.4. An axial force acting along a circle.

We consider axisymmetric deformations of an elastic transversely isotropic solid. That is, the displacements and stresses treated here are independent of angle θ in cylindrical coordinates (r,θ,z). We restrict our attention to the determination of singular stresses at the crack tip, since these are the quantities of greatest physical interest. Due to the symmetry (Fig.5) or antisymmetry (Fig.6) of the problem, it can be reduced to a mixed boundary value problem for half - space with the following mixed boundary conditions:

- for a penny-shaped crack $(r:0\le r\le a)$

$$u_z=0, \quad r>a, \quad z=0, \quad \sigma_z=0, \quad r<a, \quad z=0, \tag{2.2a}$$

$$u_r=0, \quad r>a, \quad z=0, \quad \sigma_{zr}=0, \quad r<a, \quad z=0, \tag{2.2b}$$

$$u_\theta=0, \quad r>a, \quad z=0, \quad \sigma_{z\theta}=0, \quad r<a, \quad z=0, \tag{2.2c}$$

- for an external crack $(r:r\ge a)$

$$u_z=0, \quad r<a, \quad z=0, \quad \sigma_z=0, \quad r>a, \quad z=0, \tag{2.3a}$$

$$u_r=0, \quad r<a, \quad z=0, \quad \sigma_{zr}=0, \quad r>a, \quad z=0, \tag{2.3b}$$

$$u_\theta=0, \quad r<a, \quad z=0, \quad \sigma_{z\theta}=0, \quad r>a, \quad z=0, \tag{2.3c}$$

for symmetric, antisymmetric and antisymmetric torsional loading, respectively. The symmetric torsional loading yields $\sigma_{z\theta} = 0$ for $r \geq 0, z = 0$.

Suitable elasticity solutions for a cracked solid that represent unit ring loading are obtained using the theory of Hankel transforms (see, Sneddon (1972), for example). A brief derivation of the main equations is presented in the Appendix. On the basis of those fundamental solutions it can be shown that the displacement and stress fields associated with the action of the concentrated axisymmetric ring forces and appropriate to solve the mixed boundary conditions (2.2 a, b, c) or (2.3 a, b, c) on the plane where the crack exists are as follows:

(i) For axial and radial symmetric forces as shown in Figs 4, 2 and 5

$$u_z(r,0) = \frac{1}{4\pi G_z C}\left[I_3 \int_0^\infty J_0(\xi r) J_0(\xi b) H_0(\xi s_i h)\, d\xi + \right.$$
$$\left. -\upsilon_0 I_1 \int_0^\infty J_0(\xi r) J_1(\xi b) H_1(\xi s_i h)\, d\xi + \int_0^\infty A(\xi) J_0(\xi r)\, d\xi \right], \tag{2.4}$$

$$\sigma_z(r,0) = -\frac{1}{4\pi}\int_0^\infty \xi A(\xi) J_0(\xi r)\, d\xi .$$

(ii) For axial and radial antisymmetric forces as shown in Figs 4, 2 and 6

$$u_r(r,0) = \frac{1}{4\pi G_z C s_1 s_2}\left[-\upsilon_1 I_3 \int_0^\infty J_1(\xi r) J_0(\xi b) H_2(\xi s_i h)\, d\xi + \right.$$
$$\left. + I_1 \int_0^\infty J_1(\xi r) J_1(\xi b) H_3(\xi s_i h)\, d\xi + \int_0^\infty B(\xi) J_1(\xi r)\, d\xi \right], \tag{2.5}$$

$$\sigma_{zr}(r,0) = -\frac{1}{4\pi}\int_0^\infty \xi B(\xi) J_1(\xi r)\, d\xi .$$

(iii) For antisymmetric torsional force as shown in Figs 2 and 6

$$u_\theta(r,0) = \frac{1}{4\pi G_z s_3}\left[I_2 b^{-1} \int_0^\infty e^{-\xi s_3 h} J_1(\xi r) J_1(\xi b)\, d\xi + \int_0^\infty C(\xi) J_1(d\xi) \right], \tag{2.6}$$

$$\sigma_{z\theta}(r,0) = -\frac{1}{4\pi}\int_0^\infty \xi C(\xi) J_1(\xi r)\, d\xi .$$

In the solutions (2.4), (2.5) and (2.6) the following notation is used: J_ν denotes the Bessel function of the first kind of order ν; the known functions H_0, H_1, H_2 and H_3 are presented in terms of exponentials

as shown in Eqs (A11) in the Appendix, G_z denotes the shear modulus of the material in the *z*-direction and the material parameters s_i, C, υ_0 and υ_1 are given in the Appendix by Eqs (A9) and (A10).

Within the context of linear elastic fracture mechanics, the stress intensity factors are defined as

$$\begin{Bmatrix} K_I \\ K_{II} \\ K_{III} \end{Bmatrix} = \lim_{r \to a^+} \sqrt{2(r-a)} \begin{Bmatrix} \sigma_z(r,0) \\ \sigma_{zr}(r,0) \\ \sigma_{z\theta}(r,0) \end{Bmatrix}, \tag{2.7}$$

$$\begin{Bmatrix} K_I \\ K_{II} \\ K_{III} \end{Bmatrix} = \lim_{r \to a^-} \sqrt{2(a-r)} \begin{Bmatrix} \sigma_z(r,0) \\ \sigma_{zr}(r,0) \\ \sigma_{z\theta}(r,0) \end{Bmatrix}, \tag{2.8}$$

for a penny-shaped crack and an external crack, respectively.

K_I, K_{II}, K_{III} are mode I, II, III stress intensity factors (Kanninen and Popelar, 1985), respectively, corresponding to the cases (i), (ii) and (iii) of loading, respecively.

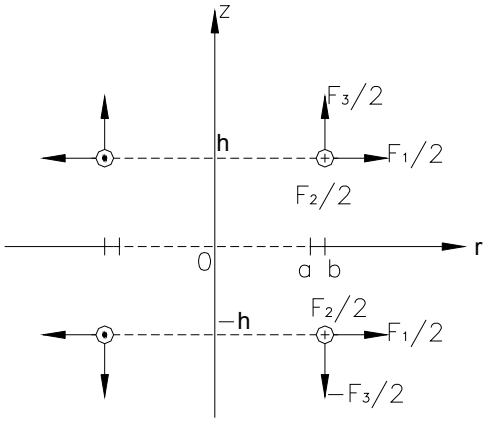

Fig.5. Symmetric loadings.

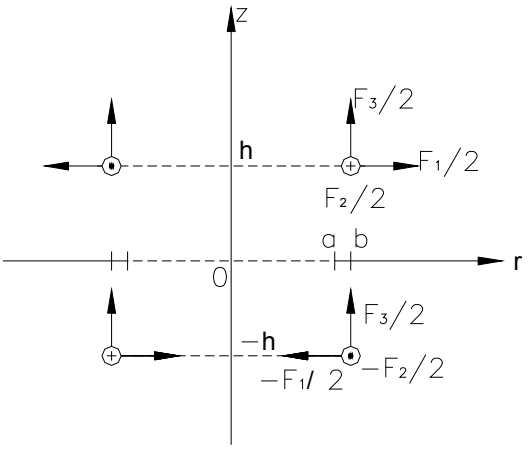

Fig.6. Antisymmetric loadings.

In the assumed axially symmetric problem, with respect to the z – axis, the torsional problem is separated and may be solved separately, as here. But in the three – dimensional case we also have another antisymmetric problem (the superposition), so that in general case the K_{II} and K_{III} will be coupled. The antisymmetric problem solution will be published separately.

3. Mode I loading

3.1. The penny-shaped crack

The boundary conditions (2.2a) and the solutions (2.4) yield

$$\begin{aligned}&\int_0^\infty A(\xi)J_0(\xi r)d\xi = -I_3\int_0^\infty J_0(\xi r)J_0(\xi b)H_0(\xi s_i h)d\xi + \\ &+\upsilon_0 I_1\int_0^\infty J_0(\xi r)J_1(\xi b)H_1(\xi s_i h)d\xi, \qquad r>a,\end{aligned} \tag{3.1}$$

$$\int_0^\infty \xi A(\xi)J_0(\xi r)d\xi = 0, \qquad r<a\,. \tag{3.2}$$

The dual integral Eqs (3.1), (3.2) are converted to the Abel integral equation by means of the following integral representation for $A(\xi)$

$$A(\xi) = \sqrt{\frac{2}{\pi}}\int_0^a g(x)\sin(\xi x)dx - I_3 J_0(\xi b)H_0(\xi s_i h) + \upsilon_0 I_1 J_1(\xi b)H_1(\xi s_i h)\,, \tag{3.3}$$

with the assumption that $g(x)\to 0$ as $x\to 0^+$.

This representation of $A(\xi)$ identically satisfies Eq.(3.1). Substitution of $A(\xi)$ into Eq.(3.2) leads to the following Abel integral equation for an auxiliary function $g(x)$

$$\begin{aligned}&\sqrt{\frac{2}{\pi}}\int_0^r \frac{dg(x)}{dx}\frac{dx}{\sqrt{r^2-x^2}} = I_3\int_0^\infty \xi J_0(\xi r)J_0(\xi b)H_0(\xi s_i h)d\xi + \\ &-\upsilon_0 I_1\int_0^\infty \xi J_0(\xi r)J_1(\xi b)H_1(\xi s_i h)d\xi.\end{aligned} \tag{3.4}$$

Applying Abel's solution method to invert the left-hand side of Eq.(3.4), the solution for $g(x)$ is obtained

$$g(x) = \sqrt{\frac{2}{\pi}}\left[I_3\int_0^\infty J_0(\xi b)\sin(\xi x)H_0(\xi s_i h)d\xi - \upsilon_0 I_1\int_0^\infty J_1(\xi b)\sin(\xi x)H_1(\xi s_i h)d\xi \right]. \tag{3.5}$$

The improper integrals in Eq.(3.5) are calculated analytically (see Appendix, Eqs (A1) and (A2)). Consequently, the auxiliary function $g(x)$ is obtained explicitly in terms of the oblate spheroidal coordinates ζ_i and η_i (see Appendix) as

$$g(x)=\sqrt{\frac{2}{\pi}}\left[\frac{I_3}{k-1}\frac{1}{x}\left(\frac{k\eta_2}{\zeta_2{}^2+\eta_2{}^2}-\frac{\eta_1}{\zeta_1{}^2+\eta_1{}^2}\right)+\right.$$
$$\left.-\frac{\upsilon_0 I_1}{ks_2-s_1}\frac{b}{x^2}\left(\frac{ks_2\zeta_1}{\left(\zeta_1{}^2+\eta_1{}^2\right)\left(1+\zeta_1{}^2\right)}-\frac{s_1\zeta_2}{\left(\zeta_2{}^2+\eta_2{}^2\right)\left(1+\zeta_2{}^2\right)}\right)\right] \tag{3.6}$$

where the material parameters s_1, s_2, k and υ_0 are given in the Appendix.

The singular part of the axial stress is given by the formula

$$\sigma_z(r,0)=\frac{1}{4\pi}\sqrt{\frac{2}{\pi}}\frac{g(a)}{\sqrt{r^2-a^2}} \qquad \text{as} \qquad r\to a+. \tag{3.7}$$

Consequently, from Eqs $(2.7)_1$, (3.6) and (3.7), the stress intensity factor at the crack tip is obtained explicitly in terms of the oblate spheroidal coordinates $\overline{\zeta}_i$ and $\overline{\eta}_i$ (the values of ζ_i and η_i for $x=a$, see the Appendix) as

$$K_I=\frac{a^{-3/2}}{2\pi^2}\left[\frac{I_3}{k-1}\left(\frac{k\overline{\eta}_2}{\overline{\zeta}_2{}^2+\overline{\eta}_2{}^2}-\frac{\overline{\eta}_1}{\overline{\zeta}_1{}^2+\overline{\eta}_1{}^2}\right)+\right.$$
$$\left.-\frac{\upsilon_0 I_1}{ks_2-s_1}\frac{b}{a}\left(\frac{ks_2\overline{\zeta}_1}{\left(1+\overline{\zeta}_1{}^2\right)\left(\overline{\zeta}_1{}^2+\overline{\eta}_1{}^2\right)}-\frac{s_1\overline{\zeta}_2}{\left(1+\overline{\zeta}_2{}^2\right)\left(\overline{\zeta}_2{}^2+\overline{\eta}_2{}^2\right)}\right)\right]. \tag{3.8}$$

3.2. An external crack

The boundary conditions (2.3a) with the use of Eq.(2.4) yield

$$\int_0^\infty A(\xi)J_0(\xi r)d\xi=-I_3\int_0^\infty J_0(\xi r)J_0(\xi b)H_0(\xi s_i h)d\xi+$$
$$+\upsilon_0 I_1\int_0^\infty J_0(\xi r)J_1(\xi b)H_1(\xi s_i h)d\xi, \qquad r<a, \tag{3.9}$$

$$\int_0^\infty \xi A(\xi)J_0(\xi r)d\xi=0, \qquad r>a. \tag{3.10}$$

The dual integral Eqs (3.9), (3.10) are converted to the Abel integral equation, by means of the following integral representation for $A(\xi)$

$$A(\xi)=\sqrt{\frac{2}{\pi}}\int_0^a f(x)\cos(\xi x)dx\,. \tag{3.11}$$

In this representation the auxiliary function $f(x)$ is assumed to be continuous over the interval [0, a]. This representation of $A(\xi)$ identically satisfies Eq.(3.10). Substitution of $A(\xi)$ into Eq.(3.9) leads to the following Abel integral equation

$$\begin{aligned}\sqrt{\frac{2}{\pi}}\int_0^r \frac{f(x)dx}{\sqrt{r^2-x^2}} &= -I_3\int_0^\infty J_0(\xi r)J_0(\xi b)H_0(\xi s_i h)d\xi + \\ &+\upsilon_0 I_1\int_0^\infty J_0(\xi r)J_1(\xi b)H_1(\xi s_i h)d\xi, \qquad r<a.\end{aligned} \tag{3.12}$$

Applying Abel's solution method, the solution for $f(x)$ is obtained

$$\begin{aligned}f(x)=\sqrt{\frac{2}{\pi}}\Bigg[&-I_3\int_0^\infty \cos(\xi x)J_0(\xi b)H_0(\xi s_i h)d\xi + \\ &+\upsilon_0 I_1\int_0^\infty \cos(\xi x)J_1(\xi b)H_1(\xi s_i h)d\xi\Bigg].\end{aligned} \tag{3.13}$$

Substituting the integrals (A3) and (A4) (see Appendix) gives the final solution for $f(x)$

$$\begin{aligned}f(x)=\sqrt{\frac{2}{\pi}}\Bigg[&-\frac{I_3}{k-1}\frac{1}{x}\left(\frac{k\zeta_2}{\zeta_2{}^2+\eta_2{}^2}-\frac{\zeta_1}{\zeta_1{}^2+\eta_1{}^2}\right)+ \\ &+\frac{\upsilon_0 I_1}{b}\left(1-\frac{1}{ks_2-s_1}\left(\frac{ks_2\eta_1\left(1+\zeta_1{}^2\right)}{\zeta_1{}^2+\eta_1{}^2}-\frac{s_1\eta_2\left(1+\zeta_2{}^2\right)}{\left(\zeta_2{}^2+\eta_2{}^2\right)}\right)\right)\Bigg]\end{aligned} \tag{3.14}$$

where the oblate spheroidal coordinates ζ_i,η_i are defined in the Appendix.

The stress $\sigma_z(r,0)$ for $r<a$ is given by

$$\sigma_z(r,0)=\frac{1}{4\pi}\sqrt{\frac{2}{\pi}}\left[\frac{f(a)}{\sqrt{a^2-r^2}}-\int_r^a \frac{df(x)}{dx}\frac{dx}{\sqrt{x^2-r^2}}\right], \qquad r<a\,. \tag{3.15}$$

Consequently, from Eqs (3.14), (3.15) and $(2.8)_1$, the stress intensity factor of mode I can be obtained in terms of the coordinates $\overline{\zeta}_i,\overline{\eta}_i$ such that

$$K_I = \frac{a^{-3/2}}{2\pi^2}\left\{\frac{I_3}{k-1}\left(\frac{k\overline{\zeta}_2}{\overline{\zeta}_2{}^2+\overline{\eta}_2{}^2}-\frac{\overline{\zeta}_1}{\overline{\zeta}_1{}^2+\overline{\eta}_1{}^2}\right)+\right.$$
$$\left.-\upsilon_0 I_1\frac{a}{b}\left[1-\frac{1}{ks_2-s_1}\left(\frac{ks_2\overline{\eta}_1\left(1+\overline{\zeta}_1{}^2\right)}{\overline{\zeta}_1{}^2+\overline{\eta}_1{}^2}-\frac{s_1\overline{\eta}_2\left(1+\overline{\zeta}_2{}^2\right)}{\left(\overline{\zeta}_2{}^2+\overline{\eta}_2{}^2\right)}\right)\right]\right\} \tag{24}$$

where $\overline{\zeta}_i$, $\overline{\eta}_i$ are obtained from ζ_i, η_i for $x = a$ (see the Appendix).

4. Mode II loading

4.1. The penny-shaped crack

Substituting the formulae (2.5) into the boundary conditions (2.2b) the following dual integral equations for antisymmetric loading cases are obtained

$$\int_0^\infty B(\xi)J_1(\xi r)d\xi = \upsilon_1 I_3\int_0^\infty J_1(\xi r)J_0(\xi b)H_2(\xi s_i h)d\xi +$$
$$-I_1\int_0^\infty J_1(\xi r)J_1(\xi b)H_3(\xi s_i h)d\xi, \qquad r > a, \tag{4.1}$$

$$\int_0^\infty \xi B(\xi)J_1(\xi r)d\xi = 0, \qquad r < a\,. \tag{4.2}$$

The integral representation for $B(\xi)$

$$B(\xi) = \xi^{1/2}\int_0^a x^{1/2}h(x)J_{3/2}(x\xi)dx +$$
$$+\upsilon_1 I_3 J_0(\xi b)H_2(\xi s_i h) - I_1 J_1(\xi b)H_3(\xi s_i h), \tag{4.3}$$

with the assumption that $x^{1/2}h(x) \to 0$ as $x \to 0+$, satisfies identically Eq.(4.1), while Eq.(4.2) is converted to the Abel integral equation

$$\sqrt{\frac{2}{\pi}}\int_0^r \frac{d\left[xh(x)\right]}{dx}\frac{dx}{\sqrt{r^2-x^2}} = -\upsilon_1 I_3 r\int_0^\infty \xi J_1(\xi r)J_0(\xi b)H_2(\xi s_i h)d\xi +$$
$$+I_1 r\int_0^\infty J_1(\xi r)J_1(\xi b)H_3(\xi s_i h)d\xi. \tag{4.4}$$

The solution of this equation is

$$h(x)=\sqrt{\frac{2}{\pi}}\left[-\upsilon_1 I_3\int_0^\infty J_0(\xi b)\left(\frac{\sin\xi x}{\xi x}-\cos\xi x\right)H_2(\xi s_i h)\,d\xi+\right.$$
$$\left.+I_1\int_0^\infty J_1(\xi b)\left(\frac{\sin\xi x}{\xi x}-\cos\xi x\right)H_3(\xi s_i h)\,d\xi\right]. \tag{4.5}$$

Using the integrals (A3) ÷ (A6) (see the Appendix) gives the final solution for the auxiliary function $h(x)$

$$h(x)=\sqrt{\frac{2}{\pi}}\left\{-\upsilon_1\frac{I_3}{x}\frac{1}{ks_2-s_1}\left[ks_2\left(\frac{\pi}{2}-\tan^{-1}\zeta_2-\frac{\zeta_2}{\zeta_2^2+\eta_2^2}\right)+\right.\right.$$
$$\left.\left.-s_1\left(\frac{\pi}{2}-\tan^{-1}\zeta_1-\frac{\zeta_1}{\zeta_1^2+\eta_1^2}\right)\right]+\frac{I_1}{b}\frac{1}{k-1}\left[\frac{k\eta_1(1-\eta_1^2)}{\zeta_1^2+\eta_1^2}-\frac{\eta_2(1-\eta_2^2)}{\zeta_2^2+\eta_2^2}\right]\right\}. \tag{4.6}$$

The singular part of the shear stress is given by

$$\sigma_{zr}(r,0)=\frac{1}{4\pi}\sqrt{\frac{2}{\pi}}\frac{a}{r}\frac{h(a)}{\sqrt{r^2-a^2}}\qquad\text{as}\qquad r\to a+. \tag{4.7}$$

Defining the stress intensity factor of mode II as in Eq.(2.8)2, and substituting $h(a)$ from Eq.(4.6) yields

$$K_{II}=\frac{a^{-3/2}}{2\pi^2}\left\{-\frac{\upsilon_1 I_3}{ks_2-s_1}\left[ks_2\left(\frac{\pi}{2}-\tan^{-1}\overline{\zeta}_2-\frac{\overline{\zeta}_2}{\overline{\zeta}_2^2+\overline{\eta}_2^2}\right)+\right.\right.$$
$$\left.\left.-s_1\left(\frac{\pi}{2}-\tan^{-1}\overline{\zeta}_1-\frac{\overline{\zeta}_1}{\overline{\zeta}_1^2+\eta_1^2}\right)\right]+\frac{I_1}{k-1}\frac{a}{b}\left[\frac{k\overline{\eta}_1(1-\overline{\eta}_1^2)}{\overline{\zeta}_1^2+\overline{\eta}_1^2}-\frac{\overline{\eta}_2(1-\overline{\eta}_2^2)}{\overline{\zeta}_2^2+\overline{\eta}_2^2}\right]\right\} \tag{4.8}$$

where $\overline{\zeta}_i$, $\overline{\eta}_i$ are the values of ζ_i, η_i for $x = a$ (see the Appendix).

4.2. An external crack

Substituting the formulae (2.5) into the boundary conditions (2.3b) the following dual integral equations for antisymmetric loading cases are obtained

$$\int_0^\infty B(\xi)J_1(\xi r)\,d\xi=\upsilon_1 I_3\int_0^\infty J_1(\xi r)J_0(\xi b)H_2(\xi s_i h)\,d\xi+$$
$$-I_1\int_0^\infty J_1(\xi r)J_1(\xi b)H_3(\xi s_i h)\,d\xi,\qquad r<a, \tag{4.9}$$

$$\int_0^\infty \xi B(\xi)J_1(\xi r)\,d\xi=0,\qquad r>a\,. \tag{4.10}$$

The integral representation for $B(\xi)$

$$B(\xi)=\sqrt{\frac{2}{\pi}}\int_0^a t(x)\sin(\xi x)\,dx\,, \tag{4.11}$$

satisfies identically Eq.(4.10), while Eq.(4.9) is converted to the Abel integral equation

$$\begin{aligned}\sqrt{\frac{2}{\pi}}\int_0^\infty \frac{xt(x)}{\sqrt{r^2-x^2}}dx &= \upsilon_1 l_3 r\int_0^\infty J_1(\xi r)J_0(\xi b)H_2(\xi s_i h)\,d\xi + \\ -l_1 r\int_0^\infty J_1(\xi r)J_1(\xi b)H_3(\xi s_i h)\,d\xi&.\end{aligned} \tag{4.12}$$

The solution of this equation is

$$\begin{aligned}t(x)=\sqrt{\frac{2}{\pi}}\Bigg[\upsilon_1 l_3\int_0^\infty J_0(\xi b)\sin(\xi x)H_2(\xi s_i h)\,d\xi + \\ -l_1\int_0^\infty J_1(\xi b)\sin(\xi x)H_3(\xi s_i h)\,d\xi\Bigg].\end{aligned} \tag{4.13}$$

Substituting the analytical formulae of the improper integrals (Eqs (A1) and (A2) in the Appendix) we get

$$\begin{aligned}t(x)=\sqrt{\frac{2}{\pi}}\Bigg[\frac{\upsilon_1 l_3}{x}\frac{1}{ks_2-s_1}\left(\frac{ks_2\eta_2}{\zeta_2^2+\eta_2^2}-\frac{s_1\eta_1}{\zeta_1^2+\eta_1^2}\right)+ \\ -\frac{l_1 b}{x^2}\frac{1}{k-1}\left(\frac{k\zeta_1}{\left(1+\zeta_1^2\right)\left(\zeta_1^2+\eta_1^2\right)}-\frac{\zeta_2}{\left(1+\zeta_2^2\right)\left(\zeta_2^2+\eta_2^2\right)}\right)\Bigg].\end{aligned} \tag{4.14}$$

The stress $\sigma_{zr}(r,0)$ is

$$\sigma_{zr}(r,0)=\sqrt{\frac{2}{\pi}}\frac{1}{4\pi}\left[-\frac{r}{\sqrt{a^2-r^2}}\frac{t(a)}{a}+r\int_r^a\frac{d\left[t(x)/x\right]}{dx}\frac{dx}{\sqrt{x^2-r^2}}\right],\qquad r<a\,. \tag{4.15}$$

The mode II stress intensity factor of an external crack is obtained as

$$\begin{aligned}K_{II}=\frac{a^{-3/2}}{2\pi^2}[-\frac{\upsilon_1 l_3}{ks_2-s_1}\left(\frac{ks_2\overline{\eta}_2}{\overline{\zeta}_2^2+\overline{\eta}_2^2}-\frac{s_1\overline{\eta}_1}{\overline{\zeta}_1^2+\overline{\eta}_1^2}\right)+ \\ +\frac{l_1}{k-1}\frac{b}{a}\left(\frac{k\overline{\zeta}_1}{\left(1+\overline{\zeta}_1^2\right)\left(\overline{\zeta}_1^2+\overline{\eta}_1^2\right)}-\frac{\overline{\zeta}_2}{\left(1+\overline{\zeta}_2^2\right)\left(\overline{\zeta}_2^2+\overline{\eta}_2^2\right)}\right).\end{aligned} \tag{4.16}$$

5. Mode III loading

5.1. The penny-shaped crack

The boundary conditions (2.2c) with the use of Eq.(2.6) yield the following dual integral equations of axisymmetric torsion of a penny-shaped crack

$$\int_0^\infty C(\xi)J_1(\xi r)d\xi = -b^{-1}I_2\int_0^\infty J_1(\xi r)J_1(\xi b)e^{-\xi s_3 h}d\xi, \qquad r > a, \tag{5.1}$$

$$\int_0^\infty \xi C(\xi)J_1(\xi r)d\xi = 0 \quad , \qquad r < a. \tag{5.2}$$

The integral representation for $C(\xi)$

$$C(\xi) = \xi^{1/2}\int_0^a x^{1/2}\phi_1(x)J_{3/2}(x\xi)d\xi - b^{-1}I_2 J_1(\xi b)e^{-\xi s_3 h}, \tag{5.3}$$

under the assumption that $x^{1/2}\phi(x) \to 0$ as $x \to 0+$, satisfies identically Eq.(5.1) and gives the Abel integral equation

$$\sqrt{\frac{2}{\pi}}\int_0^r \frac{d\left[x\phi(x)\right]}{dx}\frac{dx}{\sqrt{r^2-x^2}} = \frac{r}{b}I_2\int_0^\infty \xi J_1(\xi r)J_1(\xi b)e^{-\xi s_3 h}d\xi. \tag{5.4}$$

Applying Abel's solution method to invert the left-hand side of Eq.(5.4) and then substituting the integrals (A4) and (A6) from the Appendix give the final solution for $\phi(x)$

$$\phi(x) = \sqrt{\frac{2}{\pi}}I_2\frac{\eta_3}{x^2\left(1+\zeta_3^2\right)\left(\zeta_3^2+\eta_3^2\right)} \tag{5.5}$$

where ζ_3 and η_3 are defined in the Appendix.

The singular part of the stress $\sigma_{z\theta}$ is given by

$$\sigma_{z\theta}(r,0) = \frac{1}{4\pi}\sqrt{\frac{2}{\pi}}\frac{a}{r}\frac{\phi(a)}{\sqrt{r^2-a^2}} \qquad \text{as} \qquad r \to a+. \tag{5.6}$$

The solution (5.5) and Eq.(5.6) give

$$K_{III} = \frac{a^{-5/2}}{2\pi^2}\frac{\overline{\eta}_3}{\left(1+\overline{\zeta}_3^2\right)\left(\overline{\zeta}_3^2+\overline{\eta}_3^2\right)} \tag{5.7}$$

where $\overline{\zeta}_3$, $\overline{\eta}_3$ are the values of ζ_3, η_3 for $x = a$ (see the Appendix).

5.2. An external crack

The boundary conditions (2.3c) and the solutions (2.6) yield

$$\int_0^\infty C(\xi)J_1(\xi r)\,d\xi = -b^{-1}I_2\int_0^\infty J_1(\xi r)J_1(\xi b)e^{-\xi s_3 h}\,d\xi, \qquad r < a, \tag{5.8}$$

$$\int_0^\infty \xi C(\xi)J_1(\xi r)\,d\xi = 0, \qquad r > a. \tag{5.9}$$

These equations are formally similar to Eqs (4.9), (4.10).
Thus, the integral representation for $C(\xi)$

$$C(\xi) = \sqrt{\frac{2}{\pi}}\int_0^a \psi(x)\sin(\xi x)\,dx, \tag{5.10}$$

gives the final solution for an auxiliary function $\psi(x)$

$$\psi(x) = -\sqrt{\frac{2}{\pi}}\frac{I_2}{x^2}\frac{\zeta_3}{\left(1+\zeta_3^2\right)\left(\zeta_3^2+\eta_3^2\right)} \tag{5.11}$$

where ζ_3, η_3 are the oblate spheroidal coordinates associated with the material parameter s_3 (see the Appendix).

The stress $\sigma_{z\theta}(r,0)$ is

$$\sigma_{z\theta}(r,0) = \sqrt{\frac{2}{\pi}}\frac{1}{4\pi}\left(-\frac{r}{\sqrt{a^2-r^2}}\frac{\psi(a)}{a} + r\int_r^a \frac{d\left[\psi(x)/x\right]}{\sqrt{x^2-r^2}}\right), \qquad r < a. \tag{5.12}$$

The stress intensity factor of mode III for an external crack is given by the formula

$$K_{III} = \frac{I_2 a^{-5/2}}{2\pi^2}\frac{\overline{\zeta}_3}{\left(1+\overline{\zeta}_3^2\right)\left(\overline{\zeta}_3^2+\overline{\eta}_3^2\right)} \tag{5.13}$$

where $\overline{\zeta}_3$, $\overline{\eta}_3$ are obtained from ζ_3, η_3 for $x = a$.

6. Application

Exact solutions have been presented for the stress intensity factors of mode I, II and III at the tips of a penny – shaped crack and an external crack under axial, radial and torsional loadings. These solutions are obtained explicitly in terms of elementary functions. For any axisymmetrical distribution of those loadings of the medium with internal or external cracks the integration and / or simple superposition of the obtained results give the possibility of obtaining exact solutions for the stress intensity factors.

Example 1

We now proceed to consider some specific cases of loadings, when the axial loading $1_3/2$ and the radial loading $1_1/2$ are applied on the planes $z=\pm h$ in an annular region $b\le r\le c$ symmetrically with respect to the $z=0$ plane (see Fig.7).

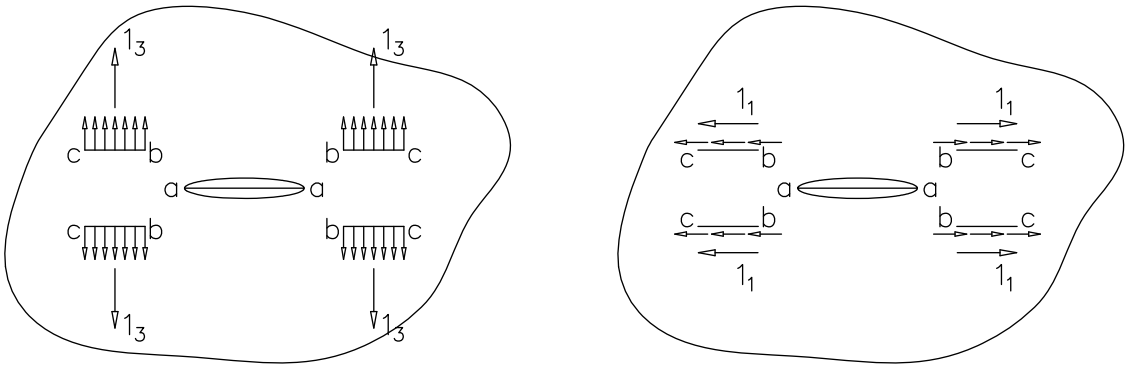

Fig.7. Axial 1_3 and radial 1_1 loadings which generate the mode I stress intensity factor K_1.

Then

$$K_1 = 2\pi\int_b^c K_1(r,h)\,r\,dr \tag{6.1}$$

where $rdr = a^2\left(\zeta^2+\eta^2\right)d\zeta/\zeta$, $d\zeta/\zeta = -d\eta/\eta$ in oblate spheroidal coordinates $r^2 = a^2\left(1+\zeta^2\right)\left(1+\eta^2\right)$, $s_0 h = a^2\zeta\eta$ and $K_{i0}(r,h)$, $K_{i1}(r,h)$ are presented in those coordinates.

From Eqs (3.8) and (6.1) we obtain for a penny – shaped crack $0\le r\le a$

$$\begin{aligned}
K_1 &= \frac{\sqrt{a}}{2\pi^2}\left[\frac{1_3}{k-1}\int_{\eta_i(b)}^{\eta_i(c)}\left(\frac{k\eta_2}{\zeta_2^2+\eta_2^2}-\frac{\eta_1}{\zeta_1^2+\eta_1^2}\right)\left[\left(-\frac{\zeta_2+\eta_2^2}{\eta_2}d\eta_2\right)\ \text{ or }\ \left(-\frac{\zeta_1+\eta_1^2}{\eta_1}d\eta_1\right)\right]+\right.\\
&-\frac{v_0 1_1}{ks_2-s_1}\frac{b}{a}\left.\int_{\zeta_i(b)}^{\zeta_i(c)}\left[\frac{ks_2\zeta_1}{\left(1+\zeta_1^2\right)\left(\zeta_1^2+\eta_1^2\right)}\left(\zeta_1^2+\eta_1^2\right)\frac{d\zeta_1}{\zeta_1}-\frac{s_1\zeta_2}{\left(1+\zeta_2^2\right)\left(\zeta_2^2+\eta_2^2\right)}\frac{\zeta_2^2+\eta_2^2}{\zeta_2}d\zeta_2\right]\right| =\\
&= \frac{\sqrt{a}}{2\pi^2}\left\{\frac{1_3}{k-1}\left[k\eta_2\left((b)-\eta_2(c)\right)-\eta_1(b)+\eta_1(c)\right]+\right.\\
&\left.-\frac{v_0 1_1}{ks_2-s_1}\frac{b}{a}\left[ks_2\left(\tan^{-1}\zeta_1(c)-\tan^{-1}\zeta_1(b)\right)-s_1\left(\tan^{-1}\zeta_2(c)-\tan^{-1}\zeta_2(b)\right)\right]\right.
\end{aligned} \tag{6.2}$$

where

$$\zeta_i(r)=\frac{1}{a\sqrt{2}}\sqrt{\sqrt{\left(r^2+s_i^2h^2-a^2\right)^2+4a^2s_i^2h^2}+r^2+s_i^2h^2-a^2},$$
$$\eta_i(r)=\frac{1}{a\sqrt{2}}\sqrt{\sqrt{\left(r^2+s_i^2h^2-a^2\right)^2+4a^2s_i^2h^2}-\left(r^2+s_i^2h^2-a^2\right)}\quad i=1,2. \tag{6.3}$$

For an external crack $r\geq a$ we have

$$\begin{aligned}K_I=\frac{\sqrt{a}}{2\pi^2}\Bigg\{&\frac{I_3}{k-1}\Big[k\zeta_2\big((c)-\zeta_2(b)\big)-\zeta_1(c)+\zeta_1(b)\Big]+\\&-v_0I_1\frac{b}{a}\Bigg[\frac{b^2-c^2}{a^2}-\frac{1}{ks_2-s_1}\left(ks_1s_2z\left(\frac{1}{\zeta_1(c)}-\frac{1}{\zeta_1(b)}-\zeta_1(c)+\zeta_1(b)\right)\right)+\\&-s_1s_2h\left(\frac{1}{\zeta_2(c)}-\frac{1}{\zeta_2(b)}-\zeta_2(c)+\zeta_2(b)\right)\Bigg].\end{aligned} \tag{6.4}$$

In special cases K_I assumes the values
- for a penny – shaped crack

$$K_I=\frac{\sqrt{a}}{2\pi^2}\begin{cases}\dfrac{I_3}{k-1}\Big[k\eta_2(b)-\eta_1(b)\Big]-v_0I_1\dfrac{b}{a}\left(\dfrac{\pi}{2}-\dfrac{ks_2\tan^{-1}\dfrac{s_1h}{a}-s_1\tan^{-1}\dfrac{s_2h}{a}}{ks_2-s_1}\right), & \text{for}\quad c\to\infty\\[2ex] I_3\left(1-\dfrac{k\eta_2(c)-\eta_1(c)}{k-1}\right)-v_0I_1\dfrac{b}{a}\left(\dfrac{ks_2\tan^{-1}\zeta_1(c)-s_1\tan^{-1}\zeta_2(c)}{ks_2-s_1}\right), & \text{for}\quad b\neq 0,\ c\ \text{finite}\\[2ex] -v_0I_1\dfrac{b}{a}\left(\tan^{-1}\sqrt{\dfrac{c^2}{a^2}-1}-\tan^{-1}\sqrt{\dfrac{b^2}{a^2}-1}\right), & \text{for}\quad h=0,\quad b\geq a,\quad c>a\end{cases} \tag{6.5}$$

When the axial loading is in plane of a crack but outside of a crack surface, then K_I are zero. This coefficient exists for radial loading applied outside a crack surface in its plane. Note that if the axial loading is applied in an infinite region $r\geq 0$ on the plane $z=\pm h$, K_I is independent on h, while for radial loadings this coefficient depends on h.

Example 2

Consider the case where $I_3/2$ and $I_1/2$ is applied on the plane $z=\pm h$ in the annular region antisymmetrically with respect to the $z=0$ plane (see Fig.8).

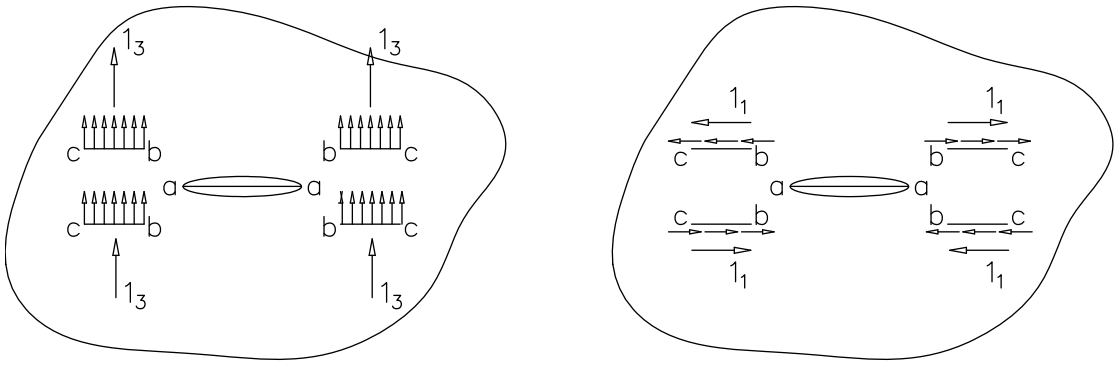

Fig.8. Axial 1_3 and radial 1_1 loadings which generate the mode II stress intensity factor K_{II}.

Then for a penny – shaped crack $(0 \le r \le a)$ we obtain from Eq.(4.8)

$$K_{II} = \frac{\sqrt{a}}{2\pi^2}\left\{-\frac{\nu_1 1_3}{k s_2 - s_1}\left[\int_{\zeta_2(b)}^{\zeta_2(c)} k s_2\left(\frac{\pi}{2} - \tan^{-1}\zeta_2 - \frac{\zeta_2}{\zeta_2^2+\eta_2^2}\right)\frac{\zeta_2^2+\eta_2^2}{\zeta_2}d\zeta_2 + \right.\right.$$
$$\left.\left. - \int_{\zeta_1(b)}^{\zeta_1(c)} s_1\left(\frac{\pi}{2} - \tan^{-1}\zeta_1 - \frac{\zeta_1}{\zeta_1^2+\eta_1^2}\right)\frac{\zeta_1^2+\eta_1^2}{\zeta_1}d\zeta_1\right] + \right. \tag{6.6}$$
$$\left. + \frac{1_1}{k-1}\frac{b}{a}\left[\int_{\eta_1(b)}^{\eta_1(c)} \frac{k\eta_1\left(1-\eta_1^2\right)}{\zeta_1^2+\eta_1^2}\left(-\frac{\zeta_1^2+\eta_1^2}{\eta_1}\right)d\eta_1 - \int_{\eta_2(b)}^{\eta_2(c)} \frac{\eta_2\left(1-\eta_2^2\right)}{\zeta_2^2+\eta_2^2}\left(-\frac{\zeta_2^2+\eta_2^2}{\eta_2}\right)d\eta_2\right]\right\},$$

$$K_{II} = \frac{\sqrt{a}}{2\pi^2}\left\{-\frac{\nu_1 1_3}{k s_2 - s_1}\left[k s_2\left(f_2(c) - f_2(b) - \zeta_2(c) + \zeta_2(b)\right) - s_1\left(f_1(c) - f_1(b) - \zeta_1(c) + \zeta_1(b)\right)\right] + \right.$$
$$\left. + \frac{1_1}{k-1}\frac{a}{b}\left[k\left(\eta_1(c) - \eta_1(b) - \frac{1}{3}\eta_1^3(c) + \frac{1}{3}\eta_1^3(b)\right) - \left(\eta_2(c) - \eta_2(b) - \frac{1}{3}\eta_2^3(c) + \frac{1}{3}\eta_2^3(b)\right)\right]\right. \tag{6.7}$$

where

$$f_i(r) = \frac{r^2}{2a^2}\left(\frac{\pi}{2} - \tan^{-1}\zeta_i + \frac{\zeta_i}{1+\zeta_i^2}\frac{1-\eta_i}{1+\eta_i}\right), \qquad i = 1,2\,. \tag{6.8}$$

For the external crack we have Eq.(4.16)

$$K_{II} = \frac{\sqrt{a}}{2\pi^2}\left\{-\frac{\nu_1 1_3}{k s_2 - s_1}\left[-k s_2\left(\eta_2(c) - \eta_2(b)\right) + s_1\left(\eta_1(c) - \eta_1(b)\right)\right] + \right.$$
$$\left. + \frac{1_1}{k-1}\frac{b}{a}\left[k\left(\tan^{-1}\zeta_1(c) - \tan^{-1}\zeta_1(b)\right) - \left(\tan^{-1}\zeta_2(c) - \tan^{-1}\zeta_2(b)\right)\right]\right. \tag{6.9}$$

Example 3

For antisymmetric torsional loading $1_2/2$ acting on the planes $z=\pm h$ (Fig.9), we obtain

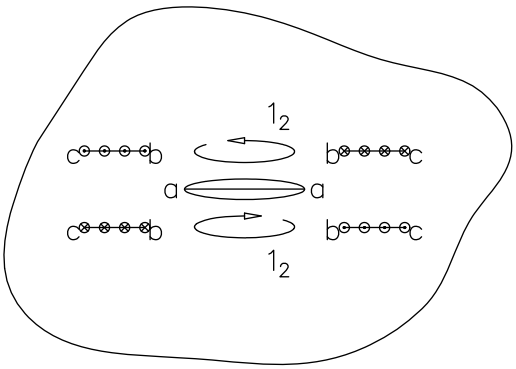

Fig.9. Torsional loadings which generate the mode III stress intensity factor K_{III}.

- for a penny – shaped crack Eq.(5.7)

$$K_{III}=\frac{1_2 a^{-1/2}}{2\pi^2}\int\limits_{\eta_3(b)}^{\eta_3(c)}\frac{\eta_3}{\left(1+\zeta_3^2\right)\left(\zeta_3^2+\eta_3^2\right)}\left(-\frac{\zeta_2^2+\eta_3^2}{\eta_3}\right)d\eta_3=\frac{1_2 a^{-1/2}}{2\pi^2}\int\limits_{\eta_3(b)}^{\eta_3(c)}\frac{d\eta_3}{1+\zeta_3^2}=$$
$$=\frac{1_2\sqrt{a}}{2\pi^2}\frac{s_3 h}{a}\left[\tan^{-1}\zeta_3(c)-\tan^{-1}\zeta_3(b)-\frac{1}{\zeta_3(c)}+\frac{1}{\zeta_2(b)}\right], \tag{6.10}$$

- for an external crack we have Eq.(5.13)

$$K_{III}=\frac{1_2 a^{-1/2}}{2\pi^2}\int\limits_{\zeta_2(b)}^{\zeta_3(c)}\frac{\zeta_3}{\left(1+\zeta_3^2\right)\left(\zeta_3^2+\eta_3^2\right)}\frac{\zeta_3^2+\eta_3^2}{\zeta_3}d\zeta_3=\frac{1_3 a^{-1/2}}{2\pi^2}\left[\tan^{-1}\zeta_3(c)-\tan^{-1}\zeta_3(b)\right]. \tag{6.11}$$

7. Numerical results

To investigate the dependence of the influence functions of a unit annular ring loadings on the stress intensity factors of mode I, II and III numerical results for the graphite – epoxy composite transversely isotropic material will be presented below. The material parameters are: $c_{11}=0.82$, $c_{12}=0.26$, $c_{13}=0.32$, $c_{33}=8.68$ and $c_{44}=0.41$ in units of 10^4MPa.

Figure 10 shows the variations of K_I^* but calculated for $1_3=1$ and $1_1=-1$. It shows that the radial loading acts in the opposite direction to the positive direction of the r – axis. Figure 11 shows the variations of non – dimensional $K_I^*=K_I\Big/\left(1_3\sqrt{a}/2\pi^2\right)$ for $1_3=1$ and $1_1=1$. A comparison of Figs 10 and 11, for a penny – shaped crack, shows that if $1_1=-1$ then the SIF increases. The radial loadings in the opposite direction to the *r* – axis give additional crack opening displacement ("buckling effect" of a penny – shaped crack).

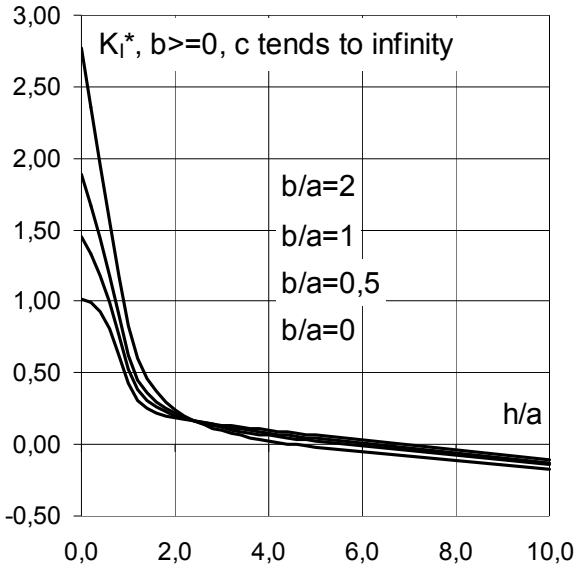

Fig.10. The variation of K_I^* with h/a for different b/a and $l_3 = 1$ and $l_1 = -1$.

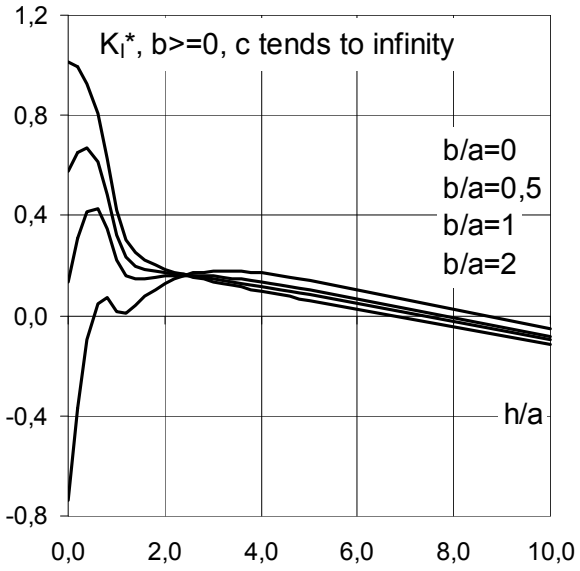

Fig.11. The variation of K_I^* with h/a for different b/a and $l_3 = 1$ and $l_1 = 1$.

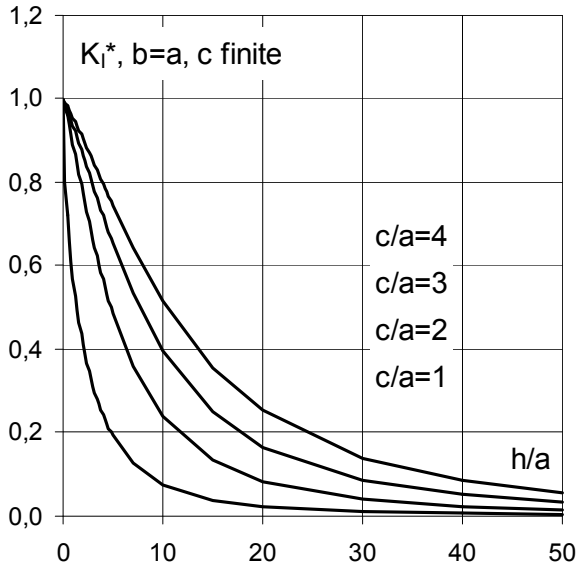

Fig.12. The variation of K_I^* with h/a for different c/a and $l_3 = 1$ and $l_1 = -1$.

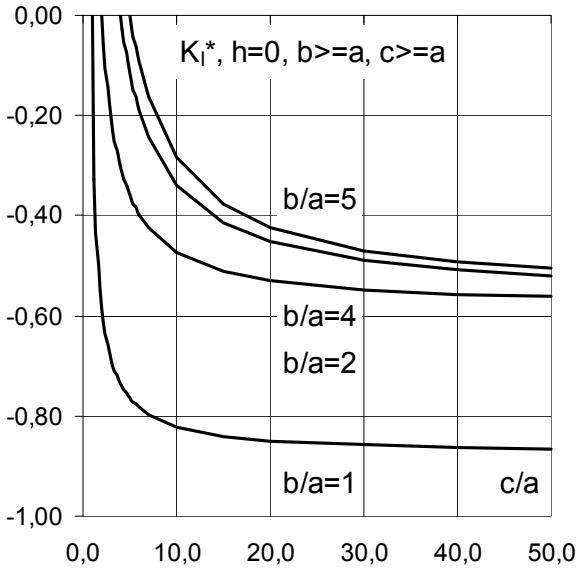

Fig.13. The variation of K_I^* with c/a for different b/a and $l_1 = 1$.

Figure 12 shows the variation of K_I^* with h/a for dissimilar annulus dimensions ($b = a$, c changes) for $l_3 = 1$ and $l_1 = -1$. Figure 13 shows K_I^* for $h = 0$, b/a, c/a change for $l_3 = 1$ (no influence) and $l_1 = 1$. In the case ($h = 0$) K_I^* (related to l_1) depends only on $l_1 = -1$ ("buckling effect"). Both Figs 12 and 13 are for a penny – shaped crack.

Figure 14 shows K_I^* versus c/a and b/a for the buckling force $1_1 = -1$. Figure 15 shows the variation of K_{II}^* for a penny – shaped crack.

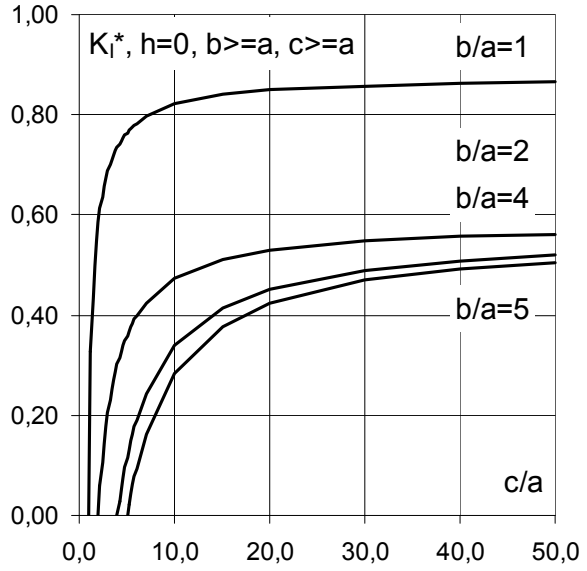

Fig.14. The variation of K_I^* with c/a and b/a for $1_1 = -1$.

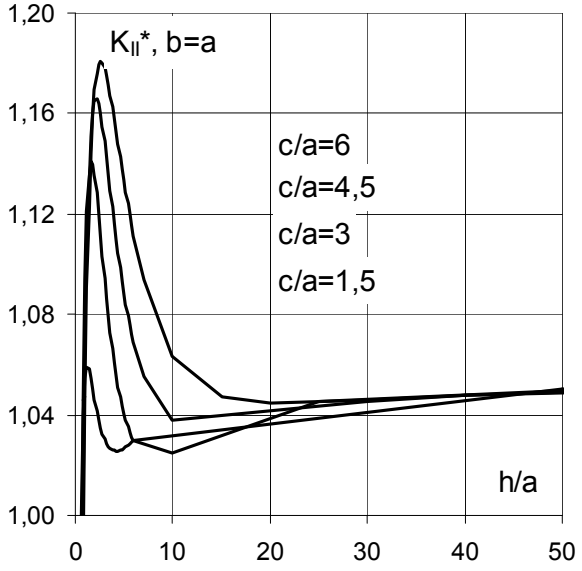

Fig.15. The variation of K_{II}^* with h/a for different c/a if $f = a$ and $1_3 = 1$, $1_1 = 1$ (penny – shaped crack).

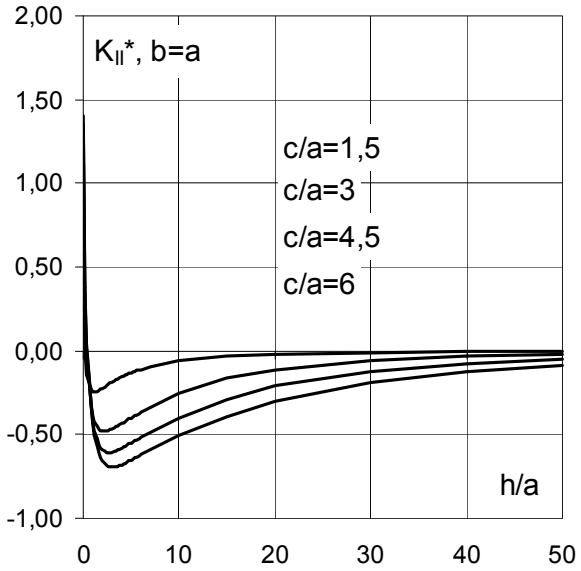

Fig.16. The variation of K_{II}^* with h/a for different c/a and $b = a$ (an external crack).

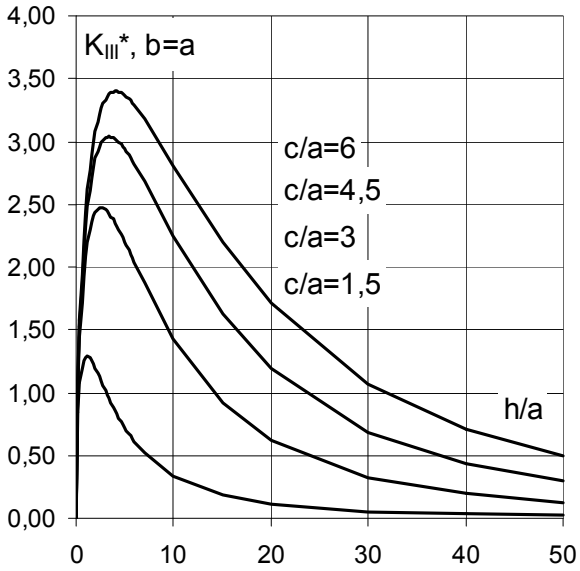

Fig.17. The variation of K_{III}^* with h/a for $b = a$ and different c/a (penny – shaped crack).

Figure 16 shows the variation of K_{II}^{*} for an external crack. In Figs 15 and 16 extreme values appear for $h/a \approx 2.5$. Figure 17 shows $K_{III}^{*} = K_{III} \Big/ \left(I_2 \sqrt{a} \Big/ 2\pi^2 \right)$ versus h/a for $b = a$ and different c/a, for a penny – shaped crack. Figure 18 shows K_{III}^{*} versus h/a for $b = a$ and different c/a, for an external crack. In the case of torsional loading the extreme value of K_{III}^{*} appears for $h/a \approx 4.0$ in the case of a penny – shaped crack.

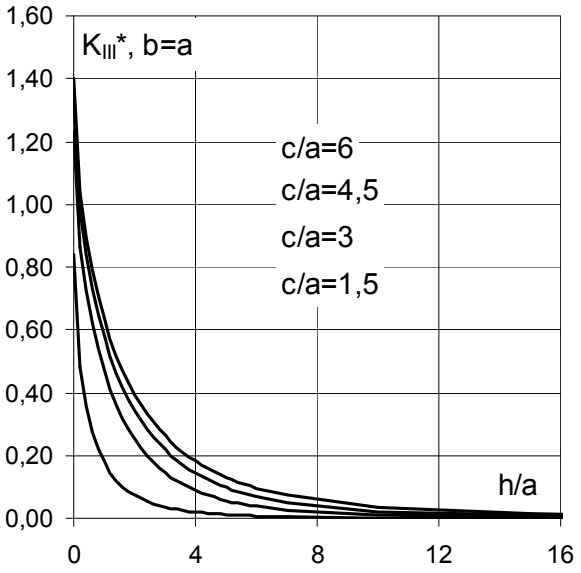

Fig.18. The variation of with h/a for $b = a$ and different c/a (an external crack).

8. Conclusions

1. Getting exact Green's functions for SIF is essential in applications because of their accuracy and computational efficiency.
2. The possibility of obtaining exact solutions in terms of elementary functions based on Green's functions constructed in this paper has not been exhausted as presented in Sections: *Application* and *Numerical Results* and three examples. We can also display a variety of other similar examples, including examples of discontinuous fields with prescribed loading sources, which can serve as a good test base for various numerical methods for solving boundary value problems of fracture mechanics.

Appendix

The following integrals are used to evaluate the auxiliary functions which appear in this paper

$$\int_0^{\infty} J_0(\xi b)\sin(\xi x) e^{-\xi s_i h} d\xi = \frac{\eta_i}{x\left(\zeta_i^2 + \eta_i^2\right)}, \tag{A1}$$

$$\int_0^{\infty} J_1(\xi b)\sin(\xi x) e^{-\xi s_i h} d\xi = \frac{b}{x^2} \frac{\zeta_i}{\left(1 + \zeta_i^2\right)\left(\zeta_i^2 + \eta_i^2\right)}, \tag{A2}$$

$$\int_0^\infty J_0(\xi b)\cos(\xi x)e^{-\xi s_i h}d\xi = \frac{\zeta_i}{x\left(\zeta_i^2+\eta_i^2\right)}, \tag{A3}$$

$$\int_0^\infty J_1(\xi b)\cos(\xi x)e^{-\xi s_i h}d\xi = \frac{1}{b}\left[1-\frac{\eta_i\left(1+\zeta_i^2\right)}{\zeta_i^2+\eta_i^2}\right], \tag{A4}$$

$$\int_0^\infty \xi^{-1}J_0(\xi b)\sin(\xi x)e^{-\xi s_i h}d\xi = \frac{\pi}{2}-\tan^{-1}\zeta_i, \tag{A5}$$

$$\int_0^\infty \xi^{-1}J_1(\xi b)\sin(\xi x)e^{-\xi s_i h}d\xi = \frac{x}{b}(1-\eta_i). \tag{A6}$$

The oblate spheroidal coordinates ζ_i, η_i are related to $b, s_i h, x$ by the equations

$$b^2 = x^2\left(1+\zeta_i^2\right)\left(1-\eta_i^2\right) \quad , \qquad s_i h = x\zeta_i\eta_i \tag{A7}$$

where $-1 \le \eta_i \le 1$ and $\zeta_i \ge 0$. The surface $\zeta_i = 0$ and $\eta_i = 0$ are respectively the interior and exterior of the circle $b = x, h = 0$; here therefore

$$\begin{aligned} &h=0, \quad b>x, \quad \zeta_i=0, \quad \eta_i=\sqrt{1-\left(b^2/x^2\right)}, \\ &h=0, \quad b<x, \quad \zeta_i=\sqrt{\left(b^2/x^2\right)-1}, \quad \eta_i=0, \\ &b=0, \quad \zeta_i=s_i h/x, \quad \eta_i=1. \end{aligned} \tag{A8}$$

The coordinates ζ_i, η_i for $x = a$ are denoted by $\overline{\zeta}_i$, $\overline{\eta}_i$.

Three sets of oblate spheroidal coordinates ζ_i, η_i ($i = 1, 2, 3$) are associated with three material parameters s_i ($i = 1, 2, 3$) which are given by equations

$$\begin{aligned} &s_1, s_2: \qquad c_{33}c_{44}s^4 - \left[c_{11}c_{33} - c_{13}\left(c_{13}+2c_{44}\right)\right]s^2 + c_{11}c_{44} = 0, \\ &\qquad\qquad s_3^2 = \left(c_{11}-c_{12}\right)/2c_{44} = G_r/G_z \end{aligned} \tag{A9}$$

where c_{ij} are five elastic constants of a transversely isotropic solid and G_r, and G_z are the shear moduli along the *r*-axis and *z*-axis, respectively; the *z*-axis is the axis of elastic symmetry of the material.

The remaining material parameters are given as

$$k=\frac{c_{33}s_1^2-c_{44}}{c_{13}+c_{44}},\qquad C=\frac{(k+1)(s_1-s_2)}{(k-1)s_1s_2},$$

$$\upsilon_0=\frac{ks_2-s_1}{(k-1)s_1s_2},\qquad \upsilon_1=\frac{ks_2-s_1}{k-1}. \tag{A10}$$

Expressions for functions $H_j(\xi s_i h)$ that appear in the analysis are as follows

$$H_0(\xi s_i h)=\frac{1}{k-1}\left(ke^{-\xi s_2 h}-e^{-\xi s_1 h}\right),$$

$$H_1(\xi s_i h)=\frac{1}{ks_2-s_1}\left(ks_2e^{-\xi s_1 h}-s_1e^{-\xi s_2 h}\right),$$

$$H_2(\xi s_i h)=\frac{1}{ks_2-s_1}\left(ks_2e^{-\xi s_2 h}-s_1e^{-\xi s_1 h}\right), \tag{A11}$$

$$H_3(\xi s_i h)=\frac{1}{k-1}\left(ke^{-\xi s_1 h}-e^{-\xi s_2 h}\right).$$

Each of these functions tend to unity as h tends to zero.
Let us consider a brief derivation of the main equations by means of Hankel transforms.

It is assumed that the geometry of the medium and the applied internal loads are axisymmetric. Therefore, one may easily separate the torsion component of the problem in which $u_\theta, \sigma_{\theta r}$ and $\sigma_{\theta z}$ are the only non zero displacement and stress components, for which

$$u_\theta=\frac{\partial\varphi_3}{\partial r},\qquad \sigma_{\theta z}=G_z\frac{\partial^2\varphi_3}{\partial r\partial z},\qquad \sigma_{r\theta}=\mathrm{G_r}\left(\frac{\partial^2\varphi_3}{\partial r^2}-\frac{1}{r}\frac{\partial\varphi_3}{\partial r}\right), \tag{A12}$$

$$\left(\nabla^2+s_3^{-2}\partial^2/\partial z^2\right)\varphi_3(r,z)=0;\qquad \nabla^2=\partial^2/\partial r^2+(1/r)\partial/\partial r, \tag{A13}$$

$$u_\theta(r,z_0-)-u_\theta(r,z_0+)=0,\qquad \sigma_{\theta z}(r,z_0-)-\sigma_{\theta z}(r,z_0+)=\frac{1_2}{4\pi r^2}\delta(r-r_0), \tag{A14}$$

$$\sigma_{\theta z}(r,0)=0\quad\text{or}\quad u_\theta(r,0)=0. \tag{A15}$$

The first condition in Eqs (A15) corresponds to symmetric and the other one to antisymmetric torsion loading with respect to the $z=0$ plane.

The solution of Eq.(A13) could be obtained through the application of Hankel integral transform. Then $\varphi_3(r,z)$ is found to be

$$\varphi_3(r,z)=\int_0^\infty \alpha^{-1}\left[A_3(\alpha)e^{\alpha s_3 z}+B_3(\alpha)e^{-\alpha s_3 z}\right]J_0(\alpha r)\,d\alpha \qquad 0\le z\le z_0,$$

$$\varphi_3(r,z)=\int_0^\infty \alpha^{-1}C_3(\alpha)e^{-\alpha s_3 z}J_0(\alpha r)\,d\alpha \qquad z_0<z. \tag{A16}$$

The conditions (A14) and (A15) yield

$$A_3=(-1)^n B_3=-\frac{1_2}{8\pi G_z s_3 r_0}e^{-\alpha s_3 z_0}J_1(\alpha r_0),$$

$$C_3=-\frac{1_2}{8\pi G_z s_3 r_0}\left(e^{\alpha s_3 z_0}+(-1)^n e^{-\alpha s_3 z_0}\right)J_1(\alpha r_0) \tag{A17}$$

where $n=0$ and $n=1$ correspond to symmetric and antisymmetric loading conditions. In deriving the results (A17) the following integral representation of the right-hand side of Eqs (A14) is used

$$\frac{1_2}{4\pi r^2}\delta(r-r_0)=\frac{1_2}{4\pi r_0}\int_0^\infty \alpha J_1(\alpha r_0)J_1(\alpha r)\,d\alpha. \tag{A18}$$

The displacement and stresses (A1) are obtained in the form

$$u_\theta(r,z)=\frac{1_2}{8\pi G_z s_3 r_0}\int_0^\infty\left(e^{-\alpha s_3(z-z_0($+(-1)^n e^{-\alpha s_3(z+z_0)}\right)J_1(\alpha r_0)J_1(\alpha r)d\alpha, \tag{A19}$$

$$\sigma_{\theta z}(r,z)=-\frac{1_2}{8\pi r_0}\int_0^\infty \alpha\left(\beta e^{-\alpha s_3(z-z_0($+(-1)^n e^{-\alpha s_3(z+z_0)}\right)J_1(\alpha r_0)J_1(\alpha r)d\alpha, \tag{A20}$$

$$\sigma_{r\theta}(r,z)=-\frac{1_2 s_3}{8\pi r_0}\int_0^\infty \alpha\left(e^{-\alpha s_3(z-z_0($+(-1)^n e^{-\alpha s_3(z+z_0)}\right)J_1(\alpha r_0)J_2(\alpha r)d\alpha \tag{A21}$$

where $\beta=\operatorname{sgn}(z-z_0)$ equals unity if $z>z_0$ and minus unity if $z<z_0$.

The remaining problem under the given internal axial and radial loads in the absence of the cracks may be solved using the displacement functions and the conditions of symmetry, continuity and discontinuity, which for axisymmetric problems may be written (Rogowski, 1975)

$$u_r=\frac{\partial}{\partial r}(k\varphi_1+\varphi_2), \qquad u_z=\frac{\partial}{\partial_z}(\varphi_1+k\varphi_2), \tag{A22}$$

$$\sigma_{rr} = -G_z(k+1)\frac{\partial^2}{\partial z^2}(\varphi_1+\varphi_2) - 2G_r\frac{1}{r}\frac{\partial}{\partial r}(k\varphi_1+\varphi_2),$$

$$\sigma_{\theta\theta} = -G_z(k+1)\frac{\partial^2}{\partial z^2}(\varphi_1+\varphi_2) - 2G_r\frac{\partial^2}{\partial r^2}(k\varphi_1+\varphi_2),$$

$$\sigma_{zz} = G_z(k+1)\frac{\partial^2}{\partial z^2}\left(s_1^{-2}\varphi_1+s_2^{-2}\varphi_2\right), \tag{A23}$$

$$\sigma_{rz} = G_z(k+1)\frac{\partial^2}{\partial r\partial z}(\varphi_1+\varphi_2),$$

$$\left(\nabla^2 + s_i^{-2}\partial^2/\partial z^2\right)\varphi_i(r,z) = 0 \qquad i = 1, 2, \tag{A24}$$

$$u_r(r,z_0-) - u_r(r,z_0+) = 0, \qquad u_z(r,z_0-) - u_z(r,z_0+) = 0, \tag{A25}$$

$$\sigma_{rz}(r,z_0-) - \sigma_{rz}(r,z_0+) = \frac{1_1}{4\pi r}\delta(r-r_0),$$

$$\sigma_{zz}(r,z_0-) - \sigma_{zz}(r,z_0+) = \frac{1_3}{4\pi r}\delta(r-r_0), \tag{A26}$$

$$u_z(r,0) = 0, \qquad \sigma_{rz}(r,0) = 0, \tag{A27}$$

or

$$u_r(r,0) = 0, \qquad \sigma_{zz}(r,0) = 0. \tag{A28}$$

The potentials $\varphi_i(r,z)$ are found to be

$$\varphi_i(r,z) = \int_0^\infty \alpha^{-1}\left[A_i(\alpha)e^{\alpha s_i z} + B_i(\alpha)e^{-\alpha s_i z}\right]J_0(\alpha r)\,d\alpha \qquad 0 \le z < z_0, \tag{A29}$$

$$\phi_i(r,z) = \int_0^\infty \alpha^{-1}C_i(\alpha)e^{-\alpha s_i z}J_0(\alpha r)\,d\alpha \qquad z_0 < z. \tag{A30}$$

The conditions (A25), (A26) and (A27) or (A28) yield

$$A_1=(-1)^n B_1=-\frac{1_3}{8\pi G_z\left(k^2-1\right)}e^{-\alpha s_1 z_0}J_1(\alpha r_0)-\frac{1_1 k}{8\pi G_z\left(k^2-1\right)s_1}e^{-\alpha s_1 z_0}J_1(\xi r_0),$$

$$A_2=(-1)^n B_2=\frac{1_3 k}{8\pi G_z\left(k^2-1\right)}e^{-\alpha s_2 z_0}J_0(\alpha r)+\frac{1_1}{8\pi G_z\left(k^2-1\right)s_2}e^{-\alpha s_2 z_0}J_1(\xi r_0),$$

(A31)

$$C_1=\frac{1_3}{8\pi G_z\left(k^2-1\right)}\left(e^{\alpha s_1 z_0}-(-1)^n e^{-\alpha s_1 z_0}\right)J_0(\alpha r_0)-\frac{1_1 k}{8\pi G_z\left(k^2-1\right)s_1}\left(e^{\alpha s_1 z_0}+(-1)^n e^{-\alpha s_1 z_0}\right)J_1(\xi r_0),$$

$$C_2=-\frac{1_3 k}{8\pi G_z\left(k^2-1\right)}\left(e^{\alpha s_2 z_0}-(-1)^n e^{-\alpha s_2 z_0}\right)J_0(\alpha r_0)+\frac{1_1}{8\pi G_z\left(k^2-1\right)s_2}\left(e^{\alpha s_2 z_0}+(-1)^n e^{-\alpha s_2 z_0}\right)J_1(\xi_0 r),$$

for symmetric $(n=0)$ and antisymmetric $(n=1)$ loading with respect to $z=0$ plane.

The displacements (A22) and stresses (A23) are

$$u_r(r,z)=-\frac{1}{8\pi G_z\left(k^2-1\right)}\left\{1_3 k\int_0^\infty\left[\beta\left(e^{-\alpha s_1|z-z_0|}-e^{-\alpha s_2|z-z_0|}\right)-(-1)^n\left(e^{-\alpha s_1(z+z_0)}+\right.\right.\right.$$
$$\left.\left.\left.-e^{-\alpha s_2(z+z_0)}\right)\right]J_0(\alpha r_0)J_1(\alpha r)d\alpha+\frac{1_1}{s_1 s_2}\int_0^\infty\left[s_1 e^{-\alpha s_2|z-z_0|}-k^2 s_2 e^{-\alpha s_1|z-z_0|}+\right.\right.$$
$$\left.\left.+(-1)^n\left(s_1 e^{-\alpha s_2(z+z_0)}-k^2 s_2 e^{-\alpha s_1(z+z_0)}\right)\right]J_1(\alpha r_0)J_1(\alpha r)d\alpha\right\},\tag{A32}$$

$$u_z(r,z)=-\frac{1}{8\pi G_z\left(k^2-1\right)}\left\{1_3\int_0^\infty\left[k^2 s_2 e^{-\alpha s_2|z-z_0|}-s_1 e^{-\alpha s_1|z-z_0|}+\right.\right.$$
$$\left.\left.-(-1)^n\left(k^2 s_2 e^{-\alpha s_2(z+z_0)}-s_1 e^{-\alpha s_1(z+z_0)}\right)\right]J_0(\alpha r_0)J_0(\alpha r)d\alpha+\right.$$
$$\left.+1_1 k\int_0^\infty\left[\beta\left(e^{-\alpha s_1|z-z_0|}-e^{-\alpha s_2|z-z_0|}\right)+(-1)^n\left(e^{-\alpha s_1(z+z_0)}-e^{-\alpha s_2(z+z_0)}\right)\right]J_1(\alpha r_0)J_0(\alpha r)d\alpha\right\},\tag{A33}$$

$$\sigma_{zz}(r,z)=\frac{1}{8\pi(k-1)}\left\{1_3\int_0^\infty\left[\beta\left(e^{-\alpha s_1|z-z_0|}-k e^{-\alpha s_2|z-z_0|}\right)+\right.\right.$$
$$\left.\left.-(-1)^n\left(e^{-\alpha s_1(z+z_0)}-k e^{-\alpha s_2(z+z_0)}\right)\right]\alpha J_0(\alpha r_0)J_0(\alpha r)d\alpha+\right.$$
$$\left.+\frac{1_1}{s_1 s_2}\int_0^\infty\left[s_1 e^{-\alpha s_2|z-z_0|}-k s_2 e^{-\alpha s_1|z-z_0|}+(-1)^n\left(s_1 e^{-\alpha s_2(z+z_0)}-k s_2 e^{-\alpha s_1(z+z_0)}\right)\right]\alpha J_1(\alpha r_0)J_0(\alpha r)d\alpha\right\},\tag{A34}$$

$$\sigma_{rz}(r,z)=\frac{1}{8\pi(k-1)}\left\{1_3\int_0^\infty\left[s_1e^{-\alpha s_1|z-z_0|}-ks_2e^{-\alpha s_2|z-z_0|}+\right.\right.$$
$$\left.-(-1)^n\left(s_1e^{-\alpha s_1(z+z_0)}-ks_2e^{-\alpha s_2(z+z_0)}\right)\right]\alpha J_0(\alpha r_0)J_1(\alpha r)d\alpha+1_1\int_0^\infty\left[\beta\left(e^{-\alpha s_2|z-z_0|}+\right.\right. \tag{A35}$$
$$\left.\left.\left.-ke^{-\alpha s_2|z-z_0|}\right)+(-1)^n\left(e^{-\alpha s_2(z+z_0)}-ke^{-\alpha s_1(z+z_0)}\right)\right]\alpha J_1(\alpha r_0)J_1(\alpha r)d\alpha\right\},$$

The stresses σ_{rr} and $\sigma_{\theta\theta}$ may be similarly expressed.

For two half-spaces problem with cracks the displacement and stress field are obtained in the forms $(z\geq 0)$

$$u_r(r,z)=-\frac{1}{G_zC(k-1)s_1s_2}\int_0^\infty C(\alpha)\left(ks_2e^{-\alpha s_1z}-s_1e^{-\alpha s_2z}\right)J_1(\alpha r)d\alpha, \tag{A36}$$

$$u_z(r,z)=\frac{1}{G_zC(k-1)}\int_0^\infty C(\alpha)\left(ke^{-\alpha s_2z}-e^{-\alpha s_1z}\right)J_0(\alpha r)d\alpha, \tag{A37}$$

$$\sigma_{zz}(r,z)=-\frac{1}{s_1-s_2}\int_0^\infty C(\alpha)\left(s_1e^{-\alpha s_2z}-s_2e^{-\alpha s_1z}\right)\alpha J_0(\alpha r)d\alpha, \tag{A38}$$

$$\sigma_{rz}(r,z)=\frac{s_1s_2}{s_1-s_2}\int_0^\infty C(\alpha)\left(e^{-\alpha s_1z}-e^{-\alpha s_2z}\right)\alpha J_1(\alpha r)d\alpha, \tag{A39}$$

for symmetric loading, i.e., $\sigma_{rz}(r,0)=0$, and

$$u_r(r,z)=\frac{1}{G_zC(k-1)s_1s_2}\int_0^\infty D(\alpha)\left(ke^{-\alpha s_1z}-e^{-\alpha s_2z}\right)J_1(\alpha r)d\alpha, \tag{A40}$$

$$u_z(r,z)=-\frac{1}{G_zC(k-1)}\int_0^\infty D(\alpha)\left(ks_2e^{-\alpha s_2z}-s_1e^{-\alpha s_1z}\right)J_0(\alpha r)d\alpha, \tag{A41}$$

$$\sigma_{zz}(r,z)=-\frac{1}{s_1-s_2}\int_0^\infty D(\alpha)\left(e^{-\alpha s_1z}-e^{-\alpha s_2z}\right)\alpha J_0(\alpha r)d\alpha, \tag{A42}$$

$$\sigma_{rz}(r,z)=\frac{1}{s_1-s_2}\int_0^\infty D(\alpha)\left(s_2e^{-\alpha s_2z}-s_1e^{-\alpha s_1z}\right)\alpha J_1(\alpha r)d\alpha, \tag{A43}$$

for antisymmetric loading, i.e., $\sigma_{zz}(r,0)=0$, and

$$u_\theta(r,z)=\frac{1}{G_z s_3}\int_0^\infty E(\alpha)e^{-\alpha s_3 z}J_1(\alpha r)d\alpha\,, \tag{A44}$$

$$\sigma_{\theta z}(r,z)=-\int_0^\infty E(\alpha)e^{-\alpha s_3 z}\alpha J_1(\alpha r)d\alpha\,, \tag{A45}$$

$$\sigma_{r\theta}(r,z)=-s_3\int_0^\infty E(\alpha)e^{-\alpha s_3 z}\alpha J_2(\alpha r)d\alpha\,, \tag{A46}$$

for antisymmetric torsion.

The solution for each half-space may be obtained as the superposition of two fields obtained above.

Nomenclature

a – radius of a penny – shaped crack or radius of bonded region for an external crack
c_{ij} – elastic constants of a transversely isotropic solid
h – the z – coordinate of applied ring forces
K_I, K_{II}, K_{III} – stress intensity factor of mode I, mode II and mode III, respectively
k – the material parameter of transversely isotropic material
r – radial coordinate
s – the eigenvalue of transversely isotropic body
u_r – radial displacement
u_θ – circumferential displacement
u_z – axial displacement
z – axial coordinate
l_1 – the resultant of radial ring force
l_2 – the resultant of circumferential ring force
l_3 – the resultant of axial ring force
ξ – Hankel parameter
ζ – oblate spheroid coordinate
η – oblate spheroid coordinate
σ – stress
θ – circumferential coordinate
υ – material parameter

References

Chung M.Y. (2014): *Green's function for an anisotropic piezoelectric half – space bonded to a thin piezoelectric layer*. – Arch. Mech., vol.66, pp.3-17, Warsaw.

Kanninen M.F. and Popelar C.H. (1985): *Advances Fracture Mechanics*. – Oxford University Press, New York; Clarendon Press, Oxford.

Kassir M.K. and Sih G.C. (1975): *Three-dimensional crack problems*. – In: Mechanics of Fracture, vol.2 (Edited by G.C. Sih), pp.44-73, Nordhoff, Leyden.

Livieri P. and Segala F. (2013): *Sharp evaluation of the Oore – Burns integral for cracks subjected to arbitrary normal stress field*. – Fatigue and Fracture of Engineering Materials and Structures, vol.37, pp.95-106, Wiley Publishing Ltd.

Muskhelishvili N.I. (1958): *Singular Integral Equations*. – Groningen, Holland. P. Noordhoff.

Nowacki J.P., Alshits V.I. and Radowicz A. (2001): *Green's function for a piezoelectric layer – substrate structure with a general line defect*. – Int. J. Appl. Electromagn. Mech., vol.14, pp.429-433.

Nowacki J.P., Alshits V.I. and Radowicz A. (2002): *2D elektro–elastic fields in a piezoelectric layer – substrate structure*. – Int. J. Engng. Sci., vol.20, pp.2057-2076.

Rogowski B. (1986): *Inclusion, punch and crack problems in an elastically supported transversely isotropic layer*. – Solid Mechanics Archives, Oxford University Press, Oxford, England, pp.65-102.

Rogowski B. (2014a): *Fracture mechanics of anisotropic bodies. Methods of analysis and solutions of crack problems*. – Lodz University of Technology, 430 pages.

Rogowski B. (2014b): *Crack problems in anisotropic thermoelasticity*. – Lodz University of Technology, 230 pages.

Sneddon I.N. and Lowengrub M. (1969): *Crack Problems in the Classical Theory of Elasticity*. – New York: Wiley.

Sneddon I.N. (1972): *The Use of Integral Transforms*. – New York: Mc Graw-Hill.

Ting T.C.T. (2007): *Mechanics of a thin anisotropic elastic layer and a layer that is bonded to anisotropic elastic body or bodies*. – Proc. R. Soc. 463, pp.2223-2239, London.

Ting T.C.T. (2008): *Green's functions for a half – space and two half – spaces bonded to a thin anisotropic elastic layer*. – J. Appl. Mech 75.

Received: September 24, 2014

Revised: March 2, 2015